



ORIGINAL ARTICLE

Oak gum mediated green synthesis of silver nanoparticles under ultrasonic conditions: Characterization and evaluation of its antioxidant and anti-lung cancer effects



Yi Cai ^a, Bikash Karmakar ^{b,*}, Huda S. AlSalem ^c, Attalla F. El-kott ^{d,e},
Mutasem Z. Bani-Fwaz ^f, Sally Negm ^{g,h}, Atif Abdulwahab A. Oyouni ^{i,j},
Osama Al-Amer ^{j,k}, Gaber El-Saber Batiha ^l

^a Department of Medical Oncology, Chinese PLA General Hospital & Medical School, Beijing 100853, China

^b Department of Chemistry, Gobardanga Hindu College, 24 Parganas (North), India

^c Department of Chemistry, College of Science, Princess Nourah bint Abdulrahman University, P. O. Box 84428, Riyadh 11671, Saudi Arabia

^d Department of Biology, College of Science, King Khalid University, Abha 61421, Saudi Arabia

^e Department of Zoology, College of Science, Damanhour University, Damanhour 22511, Egypt

^f Department of Chemistry, College of Science, King Khalid University, P.O Box 9004, Abha 61413, Saudi Arabia

^g Department of Life Sciences, Faculty of Science and Art Mahail, King Khalid University, Saudi Arabia

^h Unit of Food Bacteriology, Central Laboratory of Food Hygiene, Ministry of Health, Sharkia 44516, Egypt

ⁱ Department of Biology, Faculty of Sciences, University of Tabuk, Tabuk, Saudi Arabia

^j Genome and Biotechnology Unit, Faculty of Sciences, University of Tabuk, Tabuk, Saudi Arabia

^k Department of Medical Laboratory Technology, Faculty of Applied Medical Sciences, University of Tabuk, Tabuk, Saudi Arabia

^l Department of Pharmacology and Therapeutics, Faculty of Veterinary Medicine, Damanhour University, Damanhour 22511, AlBeheira, Egypt

Received 19 December 2021; accepted 19 March 2022

Available online 25 March 2022

KEYWORDS

Ultrasound;
Silver;
Ag NPs/O. Gum;

Abstract Herein, we represent the bio-synthesis of silver nanoparticles (Ag NPs) employing Oak gum as the green template, an efficient natural and non-toxic reductant and stabilizer based on its phytochemicals by using ultrasonic irradiation. The characterization of as-synthesized Ag NPs was performed through Fourier transformed infrared spectroscopy (FT-IR), scanning electron

* Corresponding author.

E-mail address: bkarmakar@ghcollege.ac.in (B. Karmakar).

Peer review under responsibility of King Saud University.



Production and hosting by Elsevier

Antioxidant;
Human lung cancer

microscopy (SEM), transmission electron microscopy (TEM), energy dispersive X-ray spectroscopy (EDS), elemental mapping, UV-Vis and X-ray diffraction (XRD). After the characterization, the synthesized Ag NPs/O. Gum was engaged in biological assays like study of anti-oxidant properties by DPPH mediated free radical scavenging test using MeOH and BHT as reference molecules. Thereafter, on having a significant IC_{50} value in radical scavenging assay, we extended the bio-application of the desired nanocomposite in anticancer study of A549, Calu6 and H358 human lung cell lines in-vitro through MTT assay. They had very low cell viability and high anti-human lung cancer activities dose-dependently against the cell lines without any cytotoxicity on the normal cell line (MRC-5). The IC_{50} of Ag NPs/O. Gum was found 161.25, 289.26 and 235.29 $\mu\text{g/mL}$ against A549, Calu6 and H358 cell lines, respectively. Maybe significant anti-human lung cancer potentials of Ag NPs/O. Gum against common lung cancer cell lines are related to their antioxidant activities. So, these results suggest that synthesized Ag NPs/O. Gum as a chemotherapeutic nanomaterial have a suitable anticancer activity against lung cell lines.

© 2022 The Authors. Published by Elsevier B.V. on behalf of King Saud University. This is an open access article under the CC BY-NC-ND license (<http://creativecommons.org/licenses/by-nc-nd/4.0/>).

1. Introduction

Among the different deadly human diseases cancer assumes one of the leading positions due to its invasiveness and severe mortality rate worldwide. Lung cancer is the third most common metastatic cancers after breast and prostate cancers, affecting the respiratory system in men and women. Almost 20% of the all cancer patients die of lung cancer all over the world (Bray et al., 2018; Siegel et al., 2018; Rivera et al., 2013). Engrossing different carcinogenic pollutants and mutagens, microbial infections, migration of genetic features and most importantly, anomalous human lifestyle are the most important factors in the prevalence of lung cancers (Kozower et al., 2013; Thun et al., 2008; Xue et al., 2022). Among the different conventional therapeutic strategies chemotherapy, radio therapy, targeted therapy, immunotherapy, surgery and radiosurgery are mostly followed in terms of effective inhibition and treatment (Taylor et al., 2007; Hecht, 2012; M. Stahl M., 2013; Alsharairi, 2019). However, despite the momentous success history there are several drawbacks in following these techniques. Surgery is so far considered as the best therapy in lung cancer but not quite applicable in the advanced and metastatic stages. Again, radiation or chemotherapy also involves rigorous side effects like fatigue, diarrhea, damage of nerves, toxicity, hair loss, mouth sore etc. Hence, there is urgent necessity in advanced cancer research to find out alternate formulations in combating these shortcomings (Ko et al., 2018; Jones and Baldwin, 2018).

In recent times nanotechnology, more precisely the bioengineered nanomaterials has come into prominence as advanced featured biodegradable materials for assorted medicinal applications including the diagnosis of different ailments and their treatments (Jones and Baldwin, 2018; Horikoshi and Serpone, 2013; Almeida et al., 2014; Chow and Ho, 2013; Baetke et al., 2015; Thanh and Green, 2010; Avval et al., 2020; Wu et al., 2019). In particular, the bioinspired or biogenic noble metal nanoparticles (NPs) have been used quite frequently in the treatment of cancer (Abdel-Fattah and G. W. Ali, J. Appl., 2018; Patil and Kim, 2017; Bisht and Rayamajhi, 2016; Hassanien et al., 2018; Nakkala et al., 2016; Abel et al., 2016). Different natural resources including the plant extracts (fruit, flower, bark, seed, leaves, gum etc) are exploited in the synthesis as well as modification of these green nanomaterials. The multifunctional phytochemical content in the extract have incredible ability to immobilize the noble metal ions as well as their sustainable reduction to nanosized functional particles. The phytochemical template facilitates the uniform synthesis with fantastic uniform distribution. By size these biocompatible NPs are quite close to biomolecular cells which help them to penetrate or interact within the structure. In addition, the biogenic noble NPs are exceptionally stable, having very good catalytic activity, low dielectric constant, excellent capacity to absorb infrared and ultraviolet light and exhibits very good antibacterial properties

(Mohammadinejad et al., 2016; Machado et al., 2013; Lopez-Tellez et al., 2013; Kumar et al., 2013; Kharissova et al., 2013; Sharma et al., 2015; Nadagouda et al., 2014; Sarmah et al., 2019; Vishnukumar et al., 2017; Sun et al., 2014). Recently, Food and Drug Administration department (FDA), USA has approved the use of metal NPs in therapeutic use as being safe and non-toxic.

Following up with these very informations we have been encouraged to design an Oak gum (Fig. 1) mediated Ag NPs (Ag NPs/O. Gum) under ultrasonic conditions. Oak plant belongs to *Quercus* genus and *Fagaceae* family, grows abundantly in Asia, Europe, North Africa, North, central and south America. This species produce a fruit (acorn) that has been used as traditional medicine, antiseptic and in gastrointestinal disorders. The acorn gum is rich in several phytochemicals including different phenolic acids like gallic acid, vanillic acid, ferulic acid, syringic acid and polyphenols like quercetin, kaempferol, catechin, epicatechin etc (Burlacu et al., 2020). The oxygenated biomolecules therein facilitates the immobilization of incoming Ag ions, followed by their biogenic reduction into NPs. The tiny Ag NPs have the propensity to agglomerate together which would otherwise reduce their activity. However, the plant phytochemicals help to encapsulate the NPs by electronic interactions and stabilize them by capping.

The as synthesized Ag NPs/O. Gum has been explored in the lung cancer in vitro studies over three cell lines, A549, Calu6 and H358 following MTT assay. However, the material was proved benign without any significant cytotoxicity on the normal cell line (MRC-5). As the



Fig. 1 Image of Oak Gum.

anticancer and antioxidant activity are correlated in terms of invasion mechanism, we also carried out the its antioxidant potential following DPPH radical scavenging assay.

2. Experimental

2.1. Materials and methods

The Oak fruits were purchased from local market and the gum was extracted from acorns. AgNO_3 , DPPH and all the solvents were purchased from Sigma-Aldrich and used as such. UV-Vis analyses were carried out over a Cary 100 spectrophotometer (Agilent). FT-IR was recorded over a Bruker VERTEX 80v spectrophotometer. A FESEM-TESCAN MIRA3 microscope was used for SEM analysis along with EDX detector. TEM analysis was done using a Philips CM10 microscope (200 Kv). XRD investigation was done using $\text{Co K}\alpha$ radiation ($\lambda = 1.78897 \text{ \AA}$, 40 keV, 40 mA) in the diffraction angle range of $2\theta = 5$ to 80° .

2.2. Green synthesis of Ag NPs mediated by Oak gum under sonication

As a precursor of Ag, AgNO_3 (50 mL, 1 mM) was added dropwise into an aqueous solution of Oak gum extract (10 mL, 1%) and the reaction mixture was kept with sonication at 60°C for 30 min. The progress of the reaction could be monitored by change in color to light-brown (Ag NP). After 30 min of reaction, the Ag NPs/O. Gum was recovered by centrifuge and the residue was thoroughly washed with deionized water and dried at 60°C .

2.3. Antioxidant analysis

An equal volume of DPPH free radical solution (0.04 mg/mL, 150 μL) was mixed to 5 different concentrations (31.25, 62.5, 125, 250, 500 and 1000 $\mu\text{g/mL}$) of the nanocomposite and subsequently incubated for 30 min. Absorbances of the corresponding mixtures were measured at 517 nm and the following equation was used to calculate the radical scavenging activity in terms of % inhibition.

$$\text{Inhibition}(\%) = \left(1 - \frac{\text{Abs}_{\text{sample}} - \text{Abs}_{\text{blank}}}{\text{Abs}_{\text{control}} - \text{Abs}_{\text{blank}}}\right) \times 100 \quad (1)$$

Abs sample: absorbance of the reaction mixture, Abs blank: absorbance of the blank for each sample dilution in DPPH solvent, Abs control: absorbance of DPPH solution in sample solvent.

2.4. Cytotoxicity studies by MTT assay

The cell lines were initially cultured in 96-well plates at 37°C in 5% CO_2 atmosphere for 24 h. The growth media (10% FBS) was then decanted off from the plate and were washed twice with PBS. The compounds were then introduced in different concentrations (0.5, 5, 50, 500, and 1000 $\mu\text{g/mL}$) in RPMI medium and the system was incubated again for 3 days. The MTT dye in PBS solution (10 μL , 5 mg/mL) was next added to each well and incubated again for 4 h. In the same way media was removed and replaced with 100 μL DMSO in each well. In order to assist the formazan crystal solubilization all the plates were gently swirled. Finally, absorbance of the resulting mixture was measured at 545 nm and % cell toxicity along with IC 50 were determined as the following formula.

$$\text{Toxicity}\% = \left(1 - \frac{\text{mean OD of sample}}{\text{mean OD of control}}\right) \times 100$$

$$\text{Viability}\% = 100 - \text{Toxicity}\%$$

3. Results and discussion

3.1. Characterization of the nanocomposite

A sustainable stepwise synthetic strategy was followed in the synthesis of Ag NPs/O. Gum nanocomposite. Oak gum extract containing phytochemicals initiated the toxic reagent free green reduction of Ag ions into corresponding NPs. They additionally stabilize the tiny NPs by forming a shell around them thus avoiding their coalescence. The as-synthesized nanocomposite was consequently analyzed over advanced

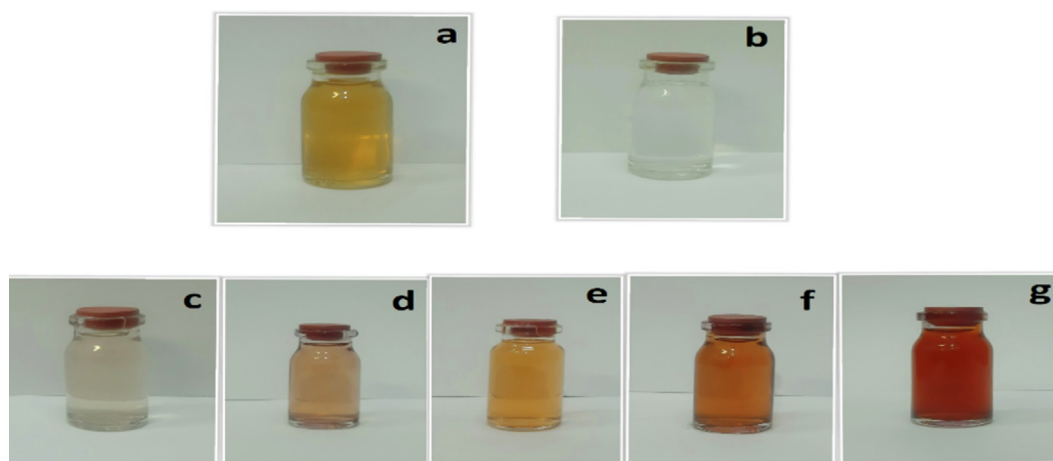


Fig. 2 Oak gum solution (a), AgNO_3 solution and color changes of synthesis Ag nanoparticles (c,d,e,f and g).

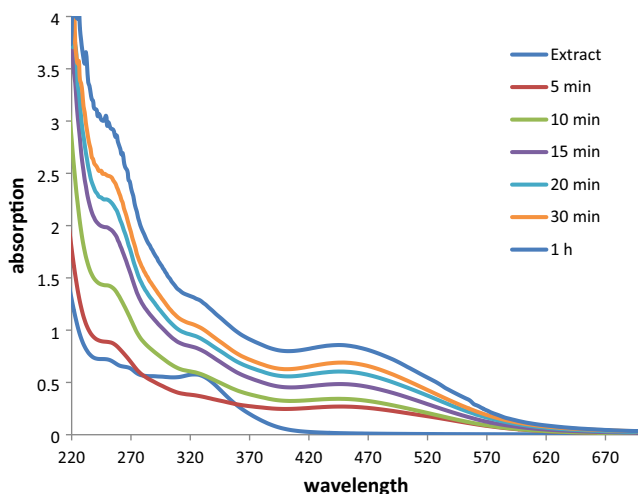


Fig. 3 Time dependant UV-Vis absorption spectra of Oak gum solution with the formation of Ag NPs.

physicochemical techniques like UV-Vis spectroscopy, TEM, EDX, elemental mapping and XRD.

The oak gum mediated reduction of Ag^+ ions into the NPs (Ag^0) can be observed visibly by change in color from colorless to deep orange, as shown in Fig. 2. UV-Vis spectrometric study was used to measure this change quantitatively when the formation of Ag NPs is detected by the characteristic Surface Plasmon Resonance (SPR) peak at 442 nm. A time dependant UV-Vis spectra has been presented in Fig. 3 where the bare extract shows absorption maxima at 330 nm. However, as soon as the Ag ions got into contact with this extract, a weak signal started generating at around 430–440 nm along

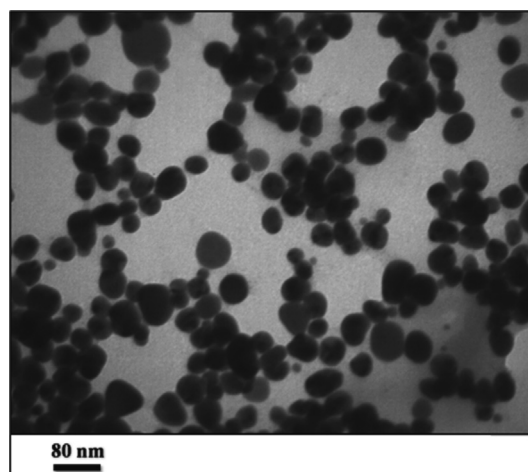


Fig. 4 TEM image of Ag NPs/O. Gum.

with the diminish of 330 nm peak. As time progressed, the new peak attributed to Ag NP evolved out sharply in 1 h of reaction time.

When it comes to assess the morphology of Ag NP@O. Gum nanocomposite, TEM analysis was carried out. Fig. 4 demonstrates the typical globular shaped Ag NPs with an average dimension of 20–30 nm. The particles are well apart and no absolute sense of agglomeration is observed. The excellent dispersion of the NPs is expected due to the NP surface functionalization by Oak phytomolecules. However, the plant modification over the NPs could not be detected from the image.

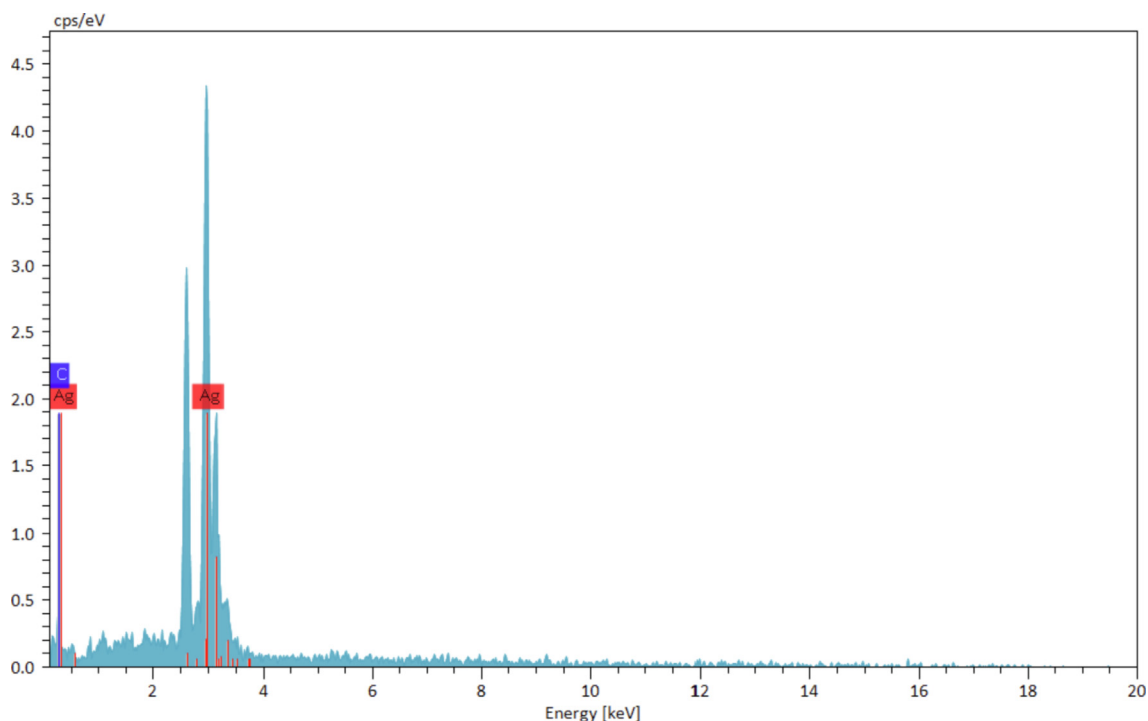


Fig. 5 EDX spectrum of Ag NPs/O. Gum.

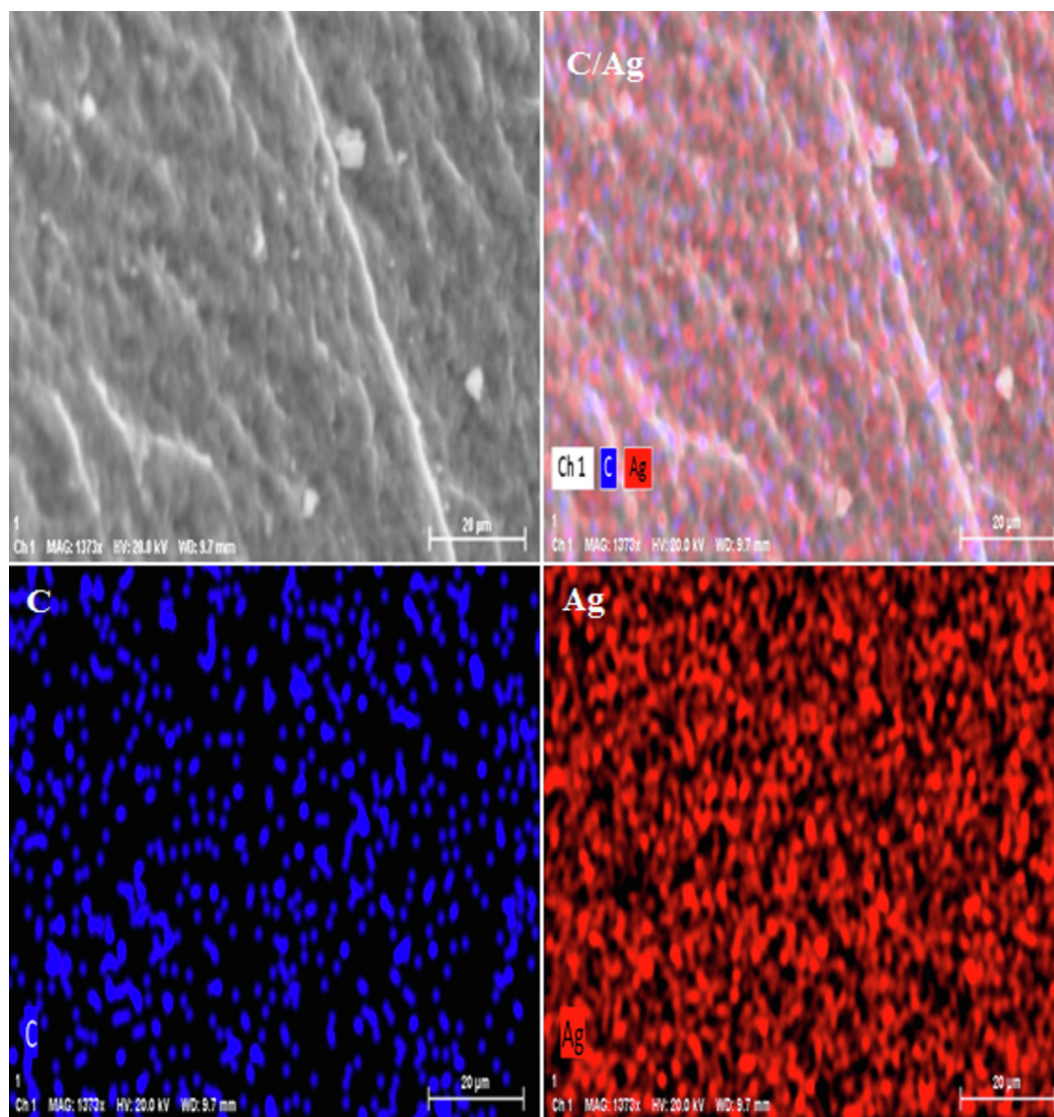


Fig. 6 SEM image of Ag NPs/O. Gum with its elemental mapping.

Chemical constitution of Ag NP@O. Gum nanocomposite was evaluated from EDX analysis Fig. 5 represents the corresponding spectrum where two sharp and characteristic signals are observed at 2.6 and 3.0 keV respectively, attributed to Ag NPs. The small peaks appeared in the lower region of the spectrum corroborates the C and O species, which indicate the O. Gum phytomolecular attachment.

SEM elemental mapping analysis was carried out to validate the EDX upshots further (Fig. 6). The nanocomposite was undergone SEM analysis followed by X-ray scanning of a small section. The outcome reveals the distribution of constituting elements with excellent dispersion throughout the matrix. Uniform distribution of Ag species, the active metal, over the surface must has a significant impact on its applications.

The crystalline nature and phase behavior of Ag NP@O. Gum nanocomposite was ascertained by XRD analysis and the outcome is displayed in Fig. 7. The single diffraction pattern indicates it as a unified moiety. Four sharp Bragg diffraction peaks are evident from the profile at $2\theta = 36.5^\circ, 43.8^\circ,$

63.2° and 74.1° , attributed to (111), (200), (220) and (311) crystallographic planes respectively. A non-crystalline broad region in the diffraction range 15 to 25° corresponds to the Oak gum phytochemicals.

3.2. Study of antioxidant potential of Ag NPs/O. Gum

While exploring the biological applications of our developed biogenic material, we started by assessing the antioxidant potential in terms of DPPH radical scavenging activity. The Ag NPs@O. Gum nanocomposite was studied in six different concentrations, such as, 31.25, 62.5, 125, 250, 500 and 1000 $\mu\text{g}/\text{mL}$ where 1:1 MeOH and BHT were considered as negative and positive controls. The DPPH free radical accepts hydride or electron from the nanocomposite and the violet color of the free ion becomes pale yellow. This visible change during the antioxidant action of the material was measured quantitatively following UV-Vis absorption (A) at 517 nm and based on those results the antioxidant property were calculated (Equation (1)). Evidently, the activity got enhanced with

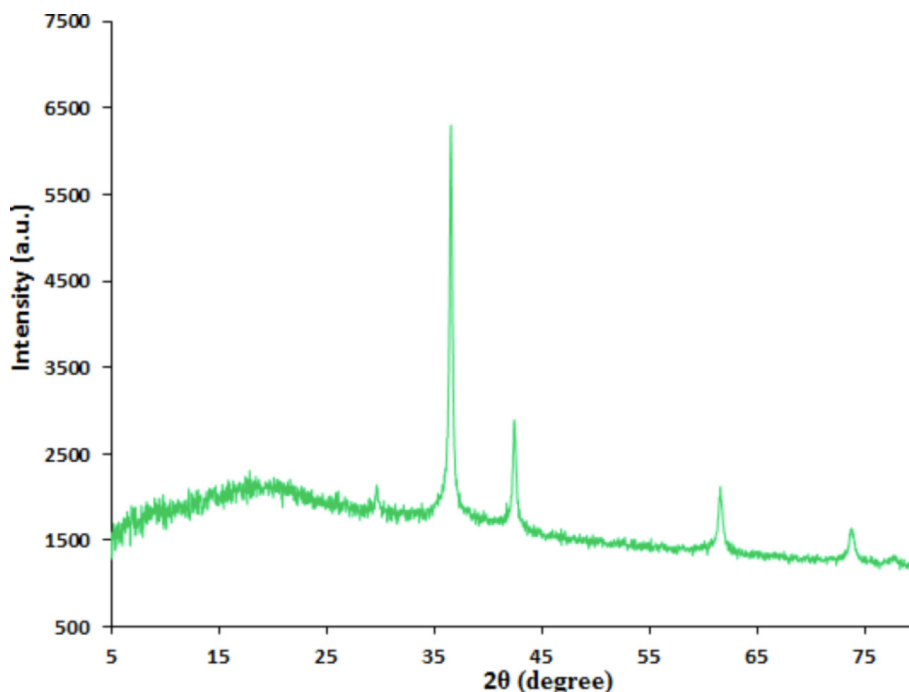


Fig. 7 XRD pattern of Ag NPs/O. Gum.

increasing the dose or sample concentration (Fig. 8) and became highest at 1000 $\mu\text{g/mL}$ (91.392%). The corresponding IC_{50} was determined as 96 $\mu\text{g/mL}$.

3.3. Cytotoxicity studies over Ag NPs/O. Gum

After having a significant IC_{50} value in the radical scavenging study in the antioxidant assay, we further explored the Ag NPs/O. Gum in the anti-lung cancer study over three standard cell lines, such as, A549, Calu6 and H358 in vitro conditions. In the cytotoxicity measurement the cells were treated in different concentrations of the nanocomposite (5–2000 $\mu\text{g/mL}$) and were investigated by MTT assay for 48 h. Interestingly, the % cell viability values over the cancer cell lines reduced with increasing doses of Ag NPs/O. Gum (Figs. 9-11). The corresponding IC_{50} values over the three cell lines were 161.25, 289.26 and 235.29 $\mu\text{g/mL}$ respectively. The cytotoxicity study was also carried on normal MRC-5 cell line which however showed insignificant % cell viability as can be seen in Fig. 12 ($\text{IC}_{50} = 2856.28$). Therefore, Ag NPs/O. Gum definitely could

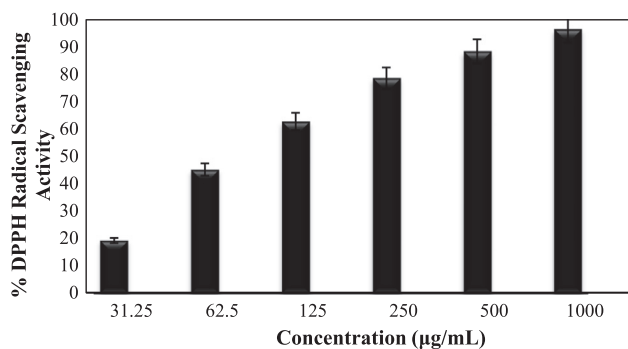


Fig. 8 Antioxidant activity of Ag NPs/O. Gum.

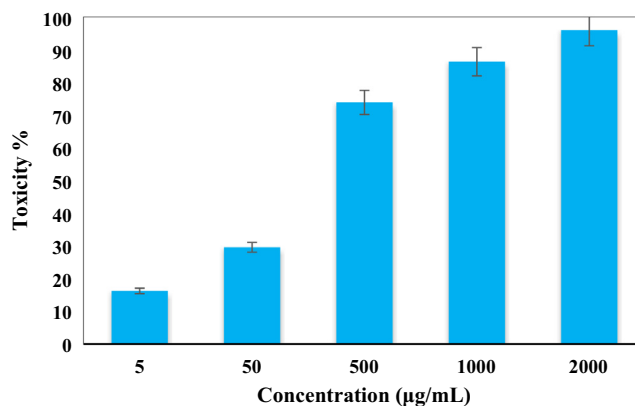


Fig. 9 *In vitro* toxicity analysis of Ag NPs/O. Gum on A549 cell line.

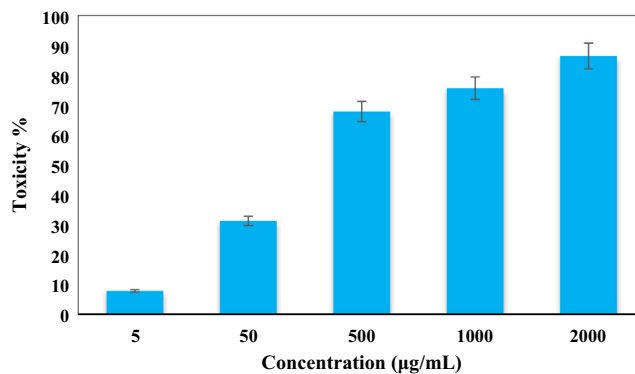


Fig. 10 *In vitro* toxicity analysis of Ag NPs/O. Gum on Calu6 cell line.

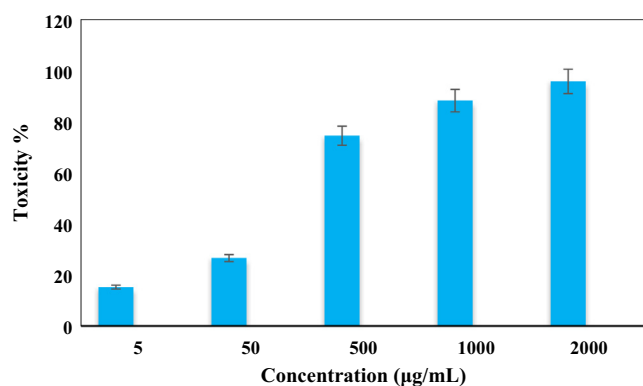


Fig. 11 *In vitro* toxicity analysis of Ag NPs/O. Gum on H358 cell line.

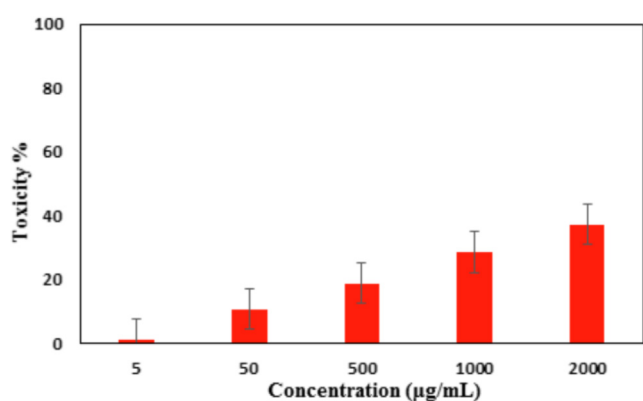


Fig. 12 *In vitro* toxicity analysis of Ag NPs/O. Gum on the normal cell line (MRC-5).

play as an efficient chemotherapeutic material against the cancer cell lines.

4. Conclusion

In conclusion, we have established herein a biogenic green process for the synthesis of Oak gum extract templated Ag NPs as a novel biocompatible nanocomposite material. The phenol acids and polyphenolic contents of Oak gum promote the green reduction of anchored Ag⁺ ions into the tiny NPs. This phytochemical adorning over the NPs also additionally stabilizes them from self-aggregation. After successful synthesis, various advanced techniques were used to characterize the Ag NPs@O. Gum nanocomposite. UV-Vis spectroscopy revealed the distinct SPR signal at around 442 nm for Ag NPs to detect. TEM analysis clearly showed the highly dispersed globular Ag NPs of 20–30 nm dimensions without visible agglomerations. The elemental composition and their surface distribution were determined by EDX and mapping analysis. It was found to be highly crystalline as indicated by the four sharp and distinct signals of Ag NPs. Towards its applications we first studied the antioxidant potential by DPPH radical scavenging investigations followed by UV-Vis analysis which revealed the IC₅₀ value as 96 µg/mL. The activity was amplified with increasing concentrations of the catalyst. On having significant antioxidant results, the material was explored furthermore in the anti-lung cancer cytotoxicity studies using standard A549, Calu6 and H358 cell lines following MTT assays. The % cell viability of the corresponding cell lines reduced dose-dependently, exhibiting IC₅₀ values as 161.25,

289.26 and 235.29 µg/mL respectively. On the other hand, it was found benevolent over the normal MRC-5 cell line. The potent results displayed by Ag NPs@O. Gum nanocomposite definitely put a significant mark in the discovery of a new formulated drug in lung cancer management.

Author contribution

All authors wrote, reviewed and edited the manuscript, analyzed the data, provided resources, were responsible for data curation, and reviewed drafts of the paper. All authors read and approved the final version of the manuscript.

Acknowledgements

This work was supported by the Princess Nourah bint Abdulrahman University, Researchers Supporting Project number (PNURSP2022R185), Princess Nourah bint Abdulrahman University, Riyadh, Saudi Arabia. Also, the authors extend their appreciation to the Deanship of Scientific Research at King Khalid University for funding this work under grant number (R. G. P2/35/43).

References

- Abdel-Fattah, W.I., Ali, G.W., 2018. *J. Appl. Biotechnol. Bioeng.* 5 (2), 00116.
- Abel, E.E., Poonga, P.R.J., Panicker, S.G., 2016. *Appl. Nanosci.* 6 (1), 121–129.
- Almeida, J.P., Lin, A.Y., Langsner, R.J., Eckels, P., Foster, A.E., Drezek, R.A., 2014. *Small* 10, 812–819.
- Alsharairi, N.A., 2019. *Nutrients* 11, 725.
- Avval, Z.M., Malekpour, L., Raeisi, F., Babapoor, A., Mousavi, S.M., Hashemi, S.A., et al. 2020. *Drug Metab. Rev.* 52, 157–184.
- Baetke, S.C., Lammers, T., Kiessling, F., 2015. *Br. J. Radiol.* 88, 0207.
- Bisht, G., Rayamajhi, S., 2016. *Nanobiomedicine* 3, 1–11.
- Bray, F., Ferlay, J., Soerjomataram, I., Siegel, R.L., Torre, L.A., Jemal, A., 2018. *CA Cancer J. Clin.* 68, 394–424.
- Burlacu, E., Nisca, A., Tanase, C., 2020. *Forests* 11, 0904.
- Chow, E.K., Ho, D., 2013. *Sci. Transl. Med.* 5, 216rv4.
- Hassanien, R., Husein, D.Z., Al-Hakkani, M.F., 2018. *Heliyon* 12, e01077.
- Hecht, S.S., 2012. *Int. J. Cancer.* 131, 2724–2732.
- Horikoshi, S., Serpone, N., 2013. *Weinheim. Wiley-VCH Verlag GmbH and Co. KGaA, Germany*, pp. 1–24.
- Jones, G.S., Baldwin, D.R., 2018. *Clin. Med.* 18 (2018), 41–46.
- Kharisova, O.V., Dias, H.V.R., Kharisov, B.I., Pérez, B.O., Pérez, V.M., 2013. *J. Biotechnol.* 31, 240–248.
- Ko, E.C., Raben, D., Formenti, S.C., 2018. *Clin. Cancer Res.* 24, 5792–5806.
- Kozower, B.D., Larner, J.M., Detterbeck, F.C., Jones, D.R., 2013. *Chest* 143, e369S–e399.
- Kumar, K.M., Mandal, B.K., Kumar, K.S., Reddy, P.S., Sreedhar, B., 2013. *Spectrochim. Acta A* 102, 128–133.
- Lopez-Tellez, G., Balderas-Hernandez, P., Barrera-Diaz, C.E., Vilchis-Nestor, A.R., Roa-Morales, G., Bilyeu, B., 2013. *J. Nanosci. Nanotechnol.* 13, 2354–2361.
- Machado, S., Pinto, S.L., Grosso, J.P., Nouws, H.P.A., Albergaria, J. T., Delerue-Matos, C., 2013. *Sci. Total Environ.* 445, 1–8.
- Mohammadinejad, R., Karimi, S., Irvani, S., Varma, R.S., 2016. *Green Chem.* 18, 20–52.
- Nadagouda, M.N., Iyanna, N., Lalley, J., Han, C., Dionysiou, D.D., Varma, R.S., 2014. *ACS Sustainable Chem. Eng.* 2, 1717–1723.
- Nakkala, J.R., Mata, R., Sadras, S.R., 2016. *Process Saf. Environ. Prot.* 100, 288–294.

- Patil, M.P., Kim, G.-D., 2017. *Appl. Microbiol. Biotechnol.* 101, 79–92.
- Rivera, M.P., Mehta, A.C., Wahidi, M.M., 2013. *Chest* 143, e142S–e165.
- Sarmah, M., Neog, A.B., Boruah, P.K., Das, M.R., Bharali, P., Bora, U., 2019. *ACS Omega* 4, 3329–5340.
- Sharma, D., Kanchi, S., Bisetty, K., 2015. *Arab. J. Chem.* 12 (8), 3576–3600.
- Siegel, R.L., Miller, K.D., Jemal, A., 2018. *CA Cancer J. Clin.* 68, 7–30.
- Stahl, M. et al., 2013. *Ann. Oncol.* 24, 51–56.
- Sun, D., Zhang, G., Jiang, X., Huang, J., Jing, X., Zheng, Y., He, J., Li, Q., 2014. *J. Mater. Chem. A* 2, 1767–1773.
- Taylor, R., Najafi, F., Dobson, A., 2007. *Int. J. Epidemiol.* 36, 1048–1059.
- Thanh, N.T., Green, L.A., 2010. *Nano Today* 5, 213–230.
- Thun, M.J., Hannan, L.M., Adams-Campbell, L.L., 2008. *PLoS Med.* 5, e185.
- Vishnukumar, P., Vivekanandhan, S., Muthuramkumar, S., 2017. *ChemBioEng Rev.* 4, 18–36.
- Wu, K., Su, D., Liu, J., Saha, R., Wang, J.P., 2019. *Nanotechnology* 30, 502003.
- Xue, Y., Karmakar, B., Ke, J., Ibrahim, H.A., Awwad, N.S., Elkott, A.F., 2022. *J. Saudi Chem. Soc.* 26, 101391.